Diffusion in a nonequilibrium binary mixture of hard spheres swelling at different rates

Alexander V. Popov and Rigoberto Hernandez

Citation: J. Chem. Phys. **131**, 024503 (2009); doi: 10.1063/1.3168405
View online: http://dx.doi.org/10.1063/1.3168405
View Table of Contents: http://jcp.aip.org/resource/1/JCPSA6/v131/i2
Published by the American Institute of Physics.

Diffusion in a nonequilibrium binary mixture of hard spheres swelling at different rates

Alexander V. Popov[a] and Rigoberto Hernandez[b]
Center for Computational and Molecular Science and Technology, School of Chemistry and Biochemistry, Georgia Institute of Technology, Atlanta, Georgia 30332-0400, USA

(Received 2 March 2009; accepted 12 June 2009; published online 13 July 2009)

The nonequilibrium dynamics of a probe in a driven binary mixture of effective hard-sphere particles has been measured computationally in molecular dynamics simulations so as to obtain a better understanding of the energy and spatial correlations that persist through the coupling between the binary components. The driving of the particles is manifested through a change of the effective volume (or equivalently, diameter of the hard spheres) and each component is assumed to have a different time-dependent profile. Such a driving is possible in a suspension of one-component colloidal mesogens, for example, in which the particle volume has been seen to change with *p*H or temperature changes in the solution. It can also be realized by growing nanoparticles during a nucleation process. The full particle dynamics has been projected onto Langevin-type models of the probe motion by representing the environment using two different reservoirs and distinct bath-probe coupling coefficients with different nonstationary properties. The bath particles corresponding to each reservoir swell with time at various rates, nonsynchronously changing their volume fractions. Under the assumption of a weak bath-bath interactions, the coupling coefficients between the probe and two baths are expressed via those in the case of a simple—consisting of one bath—environment. The general form of the resulting irreversible Langevin equation is in agreement with the MD simulations of a hard sphere probe particle diffusing in the nonstationary binary mixture.
 [DOI: 10.1063/1.3168405]

I. INTRODUCTION

At the molecular scale, chemistry is often concerned with the equilibrium end points of chemical reactions, whereas at the macroscopic scale, engineering is often concerned with the processing conditions between different metastable states of materials. In a series of articles,[1–7] we started to explore the extent to which different molecular scale perturbations can drive molecular systems to exhibit dynamic and metastable properties accessible only within nonequilibrium conditions. Macroscopic properties, such as temperature, pressure, *p*H, or polymer network structure, can change with time due to molecular-scale processes such as (chemical) reactions or (physical) phase transitions. The latter in turn will be affected by macroscopic changes. Among the molecular scale observables, we focused on the characterization of the time-dependent structure and the nonequilibrium diffusion of solutes in these systems.

To this purpose, we focused on a model system consisting of a suspension of large particles—colloids—in a liquid or gas. The nonequilibrium dynamics of this metastable system can be driven by external macroscopic forces if the particles respond to said forces by changing shape, volume or structure. Such a response can be realized by nanoparticles whose equilibrium nucleation is sensitive to solvent conditions. It can also be realized in solutions of colloidal and microgel particles that alter their size in response to temperature and *p*H changes.[8–15] The particle volumes can swell by as much as an order in magnitude in a few milliseconds,[9,16,17] thereby quickly changing the properties of the medium. Such environmental changes evidently affect the local and global structures in the suspension and give rise to nonstationarity in the diffusional motion of solutes within the suspension.

In previous work,[3,4] we have seen that the dynamics of a probe (solute) within a suspension of homogenous, but time varying, colloidal particles can be described using a reduced-dimensional model in which the solvent can be characterized as a single effective bath. In the current work, we investigate the question of how the dynamics is affected by the presence of heterogeneous colloidal particles as would be manifested within a binary mixture. The corresponding reduced dimensional model in the general case of a multinomial mixture consists of a small-dimensional system immersed in a nonequilibrium bath (see Fig. 1) partitioned by several reservoirs maintained at the same temperature. In the limit that the particles of each reservoir are identical, regardless of their interaction between reservoirs, the dynamics reduces to that of a single reservoir. The single-reservoir limit is also obtained for the contrary case of strongly entangled reservoirs regardless of their structure. On the other hand, if the

[a]Permanent address: Technological Institute, Kemerovo 650056, Russia.
[b]Author to whom correspondence should be addressed. Electronic mail: hernandez@chemistry.gatech.edu.

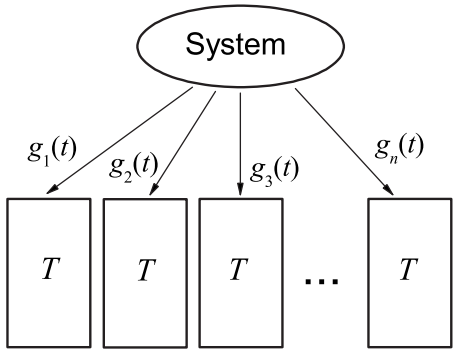

FIG. 1. A representation of a (sub)system immersed within a complex nonequilibrium environment whose interaction can be partitioned locally with respect to distinct baths (at the same temperature, T) through distinct coupling terms. The latter terms, g_i, are described in Sec. II, and enter explicitly in Eq. (2.12).

reservoirs do not interact, the dynamics of the particles respond to the reservoirs additively and the single-reservoir reduced-dimensional models can be used for each reservoir separately. The critical question answered in this work is how does the interaction between the reservoirs affect their response to the dynamics of the probe?

To be specific, we use a particle model in which a tagged sphere—the subsystem—diffuses in a binary mixture of two gases propagated by the classical equations of motion. Each gas consists of hard-sphere particles swelling with distinct but specified rates. In the limit that the solvent particles remain at constant size, the dynamics of the subsystem within this stationary environment can be accurately described by the generalized Langevin equation (GLE),[18] albeit with reference to the relative contributions of each of the components of the binary mixture. If the bath particles are driven to change size irreversibly but remain strongly and uniformly coupled to each other, then the nonstationary response of the solvent can be captured by the so-called irreversible GLE (iGLE).[1,2] In a more realistic case, one should take into account the heterogeneity of the actual bath. Use of the iLE formalism helps solve this problem by splitting the bath variables into several independent sets (reservoirs). An analogous discretization of the environment has been used in the case of spacial inhomogeneity[19,20] or when a part of the environment is prepared or maintained at nonequilibrium.[21–25] In Ref. 4, the iGLE approach has been generalized for the case of any number of nonstationary bath reservoirs with arbitrarily changing temperatures and it is summarized in Sec. II. The extension of this model to examine weakly to strongly coupled reservoirs is also described therein. The details of the numerical simulations used to explore the particle and reduced-dimensional models are described in Sec. III. The comparison between these two models in Sec. IV indicates the degree to which the coupling between the reservoirs can be captured naively from the behavior of the corresponding neat, but time-dependent, baths. The deviations arise from nonadditive interactions that appear to also contain some universality.

II. LANGEVIN DYNAMICS IN SEVERAL BATH RESERVOIRS

A. Background

When the bath is stationary, the motion of the subsystem can be accurately described by the GLE,[18]

$$\ddot{q}(t) = -\frac{\partial V(q)}{\partial q} - \int_0^t \gamma_{\mathrm{th}}(t-t')\dot{q}(t')dt' + \xi_{\mathrm{th}}(t). \tag{2.1}$$

Here $V(q)$ is the potential of mean force, $\gamma_{\mathrm{th}}(t-t')$ is the friction kernel representing the response of the solvent, $\xi_{\mathrm{th}}(t)$ is the random force due to the medium, which obeys the fluctuation-dissipation relation (FDR),

$$\langle \xi_{\mathrm{th}}(t)\xi_{\mathrm{th}}(t')\rangle = k_{\mathrm{B}}T\gamma_{\mathrm{th}}(t-t'). \tag{2.2}$$

If the bath is nonstationary, Eq. (2.1) has been modified to the so-called iGLE,[1,2] which can include both time- and space-dependent nonstationarity. In the present work, we will generally ignore the latter though it has been found to be useful in characterizing spatial inhomogeneities.[19,20] The iGLE with only time-dependent nonstationarity can be written as

$$\ddot{q}(t) = -\frac{\partial V(q)}{\partial q} - \int_0^t \gamma(t,t')\dot{q}(t')dt' + \xi(t), \tag{2.3}$$

$$\gamma(t,t') = g(t)\gamma_{\mathrm{th}}(t-t')g(t'). \tag{2.4}$$

The function $g(t)$ wrapping the friction kernel is completely determined by an irreversible behavior of the environment due to processes not otherwise included in the subsystem or bath. The stochastic force $\xi(t) \equiv g(t)\xi_{\mathrm{th}}(t)$ in the iGLE is modulated by the same amplitude $g(t)$. The resulting nonstationary FDR is

$$\langle \xi(t)\xi(t')\rangle = k_{\mathrm{B}}T\gamma(t,t'), \tag{2.5}$$

so that the temperature does not change in the course of the process.

In Ref. 2 it was shown that the iGLE can be derived from the Zwanzig-type Hamiltonian where the coupling between the chosen coordinate and the bath depends on time. This coupling is expressed via the coefficient $g(t)$, which serves as a stochastic force amplitude in Eq. (2.3). The MD simulations performed in Ref. 3 demonstrated that the diffusion of a heavy spherical particle moving among lighter ones, which swell or shrink with time, is well described by the memoryless limit of iGLE, with the function $g(t)$ determined from the velocity correlation function.

B. General memoryless limit

In previous work,[3,4] the projection of a nonequilibrium system coupled to several independent baths was shown to lead to a nonstationary stochastic equation. In the uniform temperature limit, i.e., when all the nonstationary bath reservoirs have one and the same temperature, T, as illustrated in Fig. 1, the iGLE acquires a form similar to that of Eq. (2.3) with the friction kernel

$$\gamma(t,t') = \sum_k g_k(t) g_k(t') \gamma_{(\mathrm{th})k}(t-t'), \tag{2.6}$$

where the random force correlation function obeys Eq. (2.5). The friction kernel, $\gamma_{(\mathrm{th})k}(t-t')$, represents the response of the kth bath reservoir at equilibrium, and $g_k(t)$ describes its nonstationarity multiplicative response. The initial value of the latter can be taken equal to unity, $g_k(0)=1$, without loss of generality.

In the case of diffusion of a heavy particle, the response time of the solution is negligibly small and the friction kernel acquires a memoryless form,[26]

$$\gamma_{(\mathrm{th})k}(t) = 2\gamma_{0;k}\delta(t). \tag{2.7}$$

Using it in Eq. (2.6) leads to

$$\gamma(t,t') = 2\sum_k g_k^2(t) 2\gamma_{0;k}\delta(t-t') \equiv 2\eta(t)\delta(t-t'), \tag{2.8}$$

and the iGLE (2.3) in the absence of the external potential, $V\equiv 0$, turns into the memoryless irreversible Langevin equation (iLE):

$$\ddot{q}(t) = -\eta(t)\dot{q}(t) + \xi(t), \tag{2.9a}$$

$$\langle \xi(t)\xi(t')\rangle = 2k_B T\eta(t)\delta(t-t'), \tag{2.9b}$$

where $\eta(t)$ incorporates the effects of all the environmental modes:

$$\eta(t) = \sum_k g_k^2(t)\gamma_{0;k} = G^2(t)\eta(0), \tag{2.10}$$

and $G^2(t)$ is a "weighted" stochastic force amplitude,[3]

$$G^2(t) = \frac{\Sigma\, g_k^2(t)\gamma_{0;k}}{\Sigma\, \gamma_{0;k}}. \tag{2.11}$$

Thus, in memoryless Brownian dynamics, a particle effectively diffuses in a single homogeneous environment.

Equation (2.9) can be used as the basis for describing the diffusion of a particle in an environment consisting of several baths:

$$\ddot{q}(t) = -\sum_k g_k^2(t)\gamma_{0;k}\dot{q}(t) + \sum_k \xi_k(t), \tag{2.12a}$$

$$\langle \xi_k(t)\xi_n(t')\rangle = 2k_{\mathrm{B}} T g_k^2(t)\gamma_{0;k}\delta(t-t')\delta_{k,n}, \tag{2.12b}$$

where $\delta_{k,n}$ is the discrete Kronecker delta function reflecting the independence—orthogonality—of the random forces. The coupling between the reservoirs must be neglected in order for Eq. (2.12) to be formally exact. In practice, however, the coupling (even when it is relatively strong) between pairs of particles is not sufficient to maintain correlations along a connected chain of particles that connect the tagged particle to itself through two distinct reservoirs. That is, because a diffusing particle "feels" only its immediate surroundings directly, it appears to satisfy a locality principle: Its dynamics may be fully surmised by its response to the separated influences of different subenvironments in its vicinity.

C. Two-reservoir limit

The stochastic equation of motion for a particle diffusing in two reservoirs at constant temperature T can be written in the most general form as an iLE of the form,

$$\ddot{q}(t) = -[\Gamma_1 G_1^2(t) + 2\Gamma_{12}(t) + \Gamma_2 G_2^2(t)]\dot{q}(t) + \Xi_1(t) + \Xi_2(t), \tag{2.13a}$$

where $\Xi_1(t)$ and $\Xi_2(t)$ represent the collective forces of each of the reservoirs. The interaction between the reservoirs has not been ignored and is captured in the correlation functions:

$$\langle \Xi_k(t)\Xi_k(t')\rangle = 2k_B T G_k^2(t)\Gamma_k\delta(t-t'), \quad \text{for } k\in\{1,2\}, \tag{2.13b}$$

$$\langle \Xi_1(t)\Xi_2(t')\rangle = 2k_B T\Gamma_{12}(t)\delta(t-t'). \tag{2.13c}$$

Here $\Gamma_{12}(t)$ characterizes the time-dependent coupling between two reservoirs as captured through the coupling of their collective (random) forces.

Suppose that the initial value of function $\Gamma_{12}(t)$ is negligibly small indicating there is no correlation between the two baths in the beginning. (This is exactly what is observed in the simulations described below.) Without loss of generality, we can further assume that $G_1(0)=G_2(0)=1$. It is then reasonable to introduce the frictions terms, $\gamma_{0;1}=\Gamma_1$ and $\gamma_{0;2}=\Gamma_2$, so as to construct a new equation of motion in which the reservoirs are uncoupled:

$$\ddot{q}(t) = -[\gamma_{0;1}g_1^2(t) + \gamma_{0;2}g_2^2(t)]\dot{q}(t) + \xi_1(t) + \xi_2(t), \tag{2.14a}$$

where $\xi_1(t)$ and $\xi_2(t)$ are independent (orthogonal) Gaussian forces that preserve the total force of the tagged particle, $\xi_1(t)+\xi_2(t)=\Xi_1(t)+\Xi_2(t)$. Specifically, they satisfy the correlation functions,

$$\langle \xi_k(t)\xi_k(t')\rangle = 2k_B T g_k^2(t)\gamma_{0;k}\delta(t-t') \quad \text{for } k\in\{1,2\}, \tag{2.14b}$$

$$\langle \xi_1(t)\xi_2(t')\rangle = 0. \tag{2.14c}$$

Equation (2.14a) entails the same propagation for q at $t=0$ as Eq. (2.13a).

The ensemble of trajectories generated by the stochastic equations of motion, Eqs. (2.13) and (2.14), will be the same for all time if the correlations of their respective stochastic force amplitudes are connected through the following relations:

$$g_1^2(t) = G_1^2(t) + a(t), \tag{2.15a}$$

$$g_2^2(t) = G_2^2(t) + b(t), \tag{2.15b}$$

$$a(t)\gamma_{0;1} + b(t)\gamma_{0;2} = 2\Gamma_{12}(t), \tag{2.15c}$$

where the coefficients $a(t)$ or $b(t)$ can be described as corrections to $g_1(t)$ and $g_2(t)$ due to the bath-bath interaction [note that $a(0)=b(0)=0$]. These connections are nontrivial in the sense that if it is possible to extract functions $G_k(t)$ for isolated baths from simulations or experiments then one can use them to compare with those for "orthogonal" reservoirs coupled through $g_k(t)$. In the case when a tagged particle

moves in a complex two-bath environment, then the correlation $\Gamma_{12}(t)$ between the bath reservoirs can also be extracted numerically so as to illuminate the degree to which it deviates from 0 with time (see Fig. 10 below).

The conceptual advance achieved by writing Eqs. (2.14) lies in the fact that they formalize our treatment of a two-reservoir bath as uncoupled to each other, at least, initially. That is, no matter how coupled the baths are to each other in the initial representation of Eqs. (2.13), one can always construct a new pair of baths that are uncoupled at the initial time. Such a procedure then allows one to treat the coupling perturbatively and hence enables analytical treatment. Moreover, if the system baths can be written in such a way that there exists a natural separation, then one should be able to resort to this uncoupled situation at any time with the only loss of generality being the loss of information about correlation to prior times. (Of course, if one does construct the separation transformation exactly, then one could use the formulas backward in time as well.) In what follows, we will use two baths represented by different sets of particles. At any given time, the two baths can be treated as being uncoupled instantaneously—that is, $\Gamma_{12}=0$—as a consequence of the observation of Eqs. (2.14). However, as the system is evolved, the baths will interact and recouple.

III. NUMERICAL METHODS

In the particle-scale simulations, we model the motion of a heavy tagged particle diffusing in a gas consisting of a binary mixture of 300 lighter *bath* particles. The particles interact only through hard-sphere contacts as specified by their radii. The bath particles play the role of a nonstationary environment and consists of two components, each of which represents a different bath reservoir. The nonstationarity arises because spheres in each reservoir swell with time and it is inhomogeneous because they swell at different rates, w_1 and w_2.

The entire system is propagated under NVE conditions using standard numerical integration. All of the particles are placed in a cube with sides equal to $L=2380$ nm with periodical boundary conditions. The mass of the heavy particle is $M=1.661\times10^{-13}$ g and that of gas particles is set to $m=M/50$ $(=3.321\times10^{-15}$ g). The radii r_1 and r_2 of the spheres belonging to different reservoirs 1 and 2 change linearly with time,

$$r_k = r_0 + w_k t, \quad k = 1,2, \tag{3.1}$$

where the initial radius is chosen equal to $r_0=30$ nm for all spheres. The tagged sphere radius is set to $R=100$ nm and does not change with time. Each bath reservoir contains half of the bath particles, $N_1=N_2=150$. To keep the temperature constant the total energy is constrained to be constant by requiring that the masses are invariant to the swelling and treating collisions instantaneously with respect to fixed masses and radii. To the extent that the average kinetic energy of each particle remains constant through the dynamics, the system behaves as if has a temperature satisfying equipartition at the temperature of the initial configuration, which is generally maintained at 300 K. Throughout this work, we assume that the particle systems is large enough that it can be meaningfully referred to by way of this temperature.

Four specific cases of the growth rates (w_1,w_2) have been investigated in this work. In units of nm/μs, these are (0.1,0.1), (0,0.1), (0,0.2), and (0.1,0.2). The order of magnitude of the nontrivial growth rates is somewhat larger than experimental estimates, which range from one to several tens of nanometers per millisecond.[9,27] The present choices are made deliberately: With these rates the swelling interferes in other processes strongly affecting the relaxation of the velocity autocorrelation function (VACF) so that the swelling cannot be regarded as a slow adiabatic process.

In order to compare the dynamics within the binary system to the limiting cases within neat baths, we first simulate a system consisting of 150 bath particles whose swelling rate is taken equal to the three distinct rates, $w=0$, $w=0.1$ nm/μs, and $w=0.2$ nm/μs, encompassed by the binary growth rate pairs above. As per the previous section, we use these results to obtain the amplitudes $G_k(t)$ of the "nonorthogonal" bath modes. As was shown previously for the limit of a homogeneous bath in there are no memory effects associated with the environmental response,[3] this amplitude depends only on the macrostate of the system. The latter, in turn, can be defined by any parameter, which is characteristic of either static, structural, or dynamic properties. Examples of a parameter corresponding to each of these properties are the particles' radius, the contact value of the pair correlation function, and the frequency of collisions, respectively. A simple scaling rule can be applied to calculate $G_k(t;w)$ at any w,[3]

$$G_k(t;w) = G_k(wt/w_0;w_0), \tag{3.2}$$

indicating that the product wt—which is additive to the radius—fully characterizes the instantaneous macrostate. Exploring this result, each amplitude $G_k(t;w)$ can be written in the form of a universal function depending only on the radius $r(t)$, which fully defines the state of the system:

$$G_k(t;w) \equiv G(r(t)).$$

Note also that the values of the coefficients $\gamma_{0;1}$ and $\gamma_{0;2}$ are equal to each other because they represent the initial dissipative forces corresponding to each bath reservoirs and these are identical at the beginning. Their values, $\gamma_{0;1}=\gamma_{0;2}=6.25\times10^4$ s^{-1}, for the specific realization of the particle model under investigation here have been obtained from the numerical simulations and exactly corresponds to the Enskog theory[28] in the case of small volume fraction.

The amplitudes $g_k(t)$ and $G_k(t)$ can be extracted from the VACFs of the particle model,

$$C(t_0,t) \equiv \frac{\langle \mathbf{v}(t_0)\cdot\mathbf{v}(t)\rangle}{\langle \mathbf{v}^2(t_0)\rangle}. \tag{3.3}$$

The corresponding VACFs in the iLE were shown in Ref. 3 to take the form,

$$C_{w_k}(t_0,t) = \exp\left[-\int_{t_0}^{t} \gamma_{0;k} G_k^2(t')dt' \right], \tag{3.4}$$

for the one-bath model. The VACF for the two-bath model follows similarly from Eqs. (2.14). The effective two-bath friction term, $(\gamma_{0;1}g_1^2(t') + \gamma_{0;2}g_2^2(t'))$, therein plays the role of $\gamma_{0;k}G_k^2(t')$ in the one-bath equation of motion. It follows that the VACF is

$$C_{w_1,w_2}(t_0,t) = \exp\left[-\int_{t_0}^{t} (\gamma_{0;1}g_1^2(t') + \gamma_{0;2}g_2^2(t'))dt' \right] \tag{3.5}$$

for the two-bath model, where the indices w_1 and w_2 denote the one- and two-dimensional parameterizations of the growth rates in the respective nonequilibrium processes.

Polynomial fitting has been used to smooth the functions $\ln C(t_0,t)$. The time derivations of the fits (divided by $\gamma_{0;k}$) give the desired amplitudes. Due to large relative fluctuations of the VACFs, this procedure becomes less accurate at times which are close to the maximal simulation times, $t_{\max}$, when the volume fraction reaches $\eta \approx 0.4$. It corresponds to $t_{\max} \approx 2000$ μs for the one-bath model with the swelling rate $w=0.1$ nm/μs and varies from $t_{\max} \approx 1000$ μs to $t_{\max} \approx 2000$ μs for the two-reservoir model.

As previously noted, a particular value of the amplitude $G_k(t)$ is fully defined by the macrostate of the system. The motion of the heavy particle is determined by the statistics of collisions with the particles in the closest surroundings; the hard sphere model allows for immediate contacts only. The concentration of the bath particles in the vicinity of the tagged sphere is related to the pair correlation function, $p(r)$, whose value at the contact, p_c, defines the collision frequency, ν. In the homogeneous bath, all these quantities—r, p_c, and ν—are unambiguously connected to each other and to the state of the system. Thus, functions G_k are "one-dimensional" in the sense that a single parameter suffices to uniquely specify their form.

The situation becomes more complicated if there are two bath reservoirs consisting of particles with different radii, r_1 and r_2. The interaction between the reservoirs leads to the interrelation between such quantities as p_{1c} and p_{2c} or ν_1 and ν_2, so that they do not depend on the corresponding radii alone but also on the constituent compositions. In this case, it is reasonable to assume that the amplitudes of the stochastic forces in Eq. (2.14a), g_1 and g_2, are the functions of state of each separate reservoir, namely,

$$g_k = g_k(r_k, p_{kc}), \quad \text{or} \quad g_k = g_k(r_k, \nu_k),$$

and, hence, can be regarded as "two-dimensional" functions whose time dependence can be characterized through the specification of two such parameters.

IV. RESULTS AND DISCUSSION

A. One-reservoir response

Figure 2 depicts the VACF, $C_{w_1}(t_0,t)$, of the tagged particle diffusing in a homogeneous bath consisting of 150 spheres (one reservoir), which swell at a rate $w_1 = 0.1$ nm/μs. Also shown in the figure is the polynomial fit of this VACF, which is used for obtaining the amplitude, $G_1(t;w=0.1)$ [and $G_2(t;w=0.1)$], by inverting Eq. (3.4). The amplitudes $G_k(t;w)$ can be rescaled according to Eq. (3.2) so as to obtain them at any w.

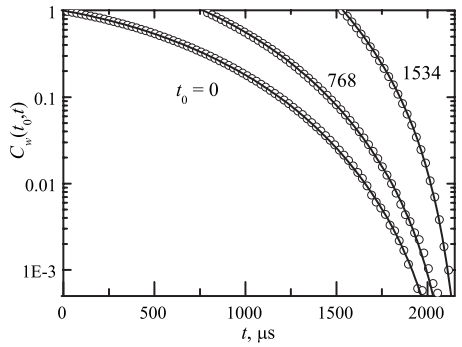

FIG. 2. The VACFs for a one-reservoir model (with 150 bath particles) at the swelling rate $w=0.1$ nm/μs are displayed at three different times, t_0. In each case, the simulation data are represented as open circles and the polynomial fits to the data are shown as solid curves.

$G_k^2(t;w=0.1)$ and the normalized frequency of collisions between the probe and the bath particles are presented in Fig. 3. The proportionality, which is seen at early times (and at small volume fractions), is in accordance with Enskog theory.[3,28] The functions $G_k(t;w)$ will be used below as reference coupling coefficients for finding the total stochastic force amplitudes in several cases of different swelling rates.

B. Two-reservoir response: One rigid and one swelling

The VACFs for a two-reservoir system with one stationary reservoir—*vis-a-vis*, with a swelling rate $w_1=0$—are shown in Fig. 4. The rate for the second reservoir is $w_2 = 0.1$ nm/μs. The contributions from the two baths are distinguishable due to the fact that the stationary particles continue to have a similar direct interaction, that is, that which does not include collisions with any other particles, with the probe while the swelling particles necessarily have a time-dependent interaction even in their direct interaction. It can be treated perturbatively because the volume fraction remains very low (~ 0.001). Moreover, the function g_1 for the stationary reservoir depends on the local enhancement only and it is directly connected to the collision frequency ν_1.

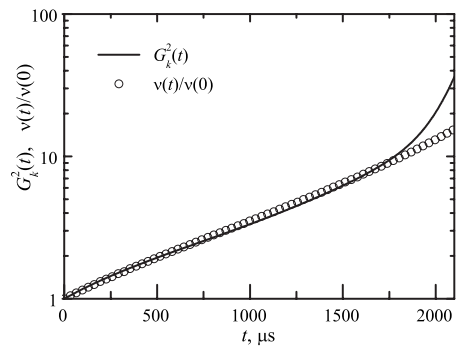

FIG. 3. $G_k^2(t)$ and $\nu(t)/\nu(0)$ are displayed vs time within the swelling regime.

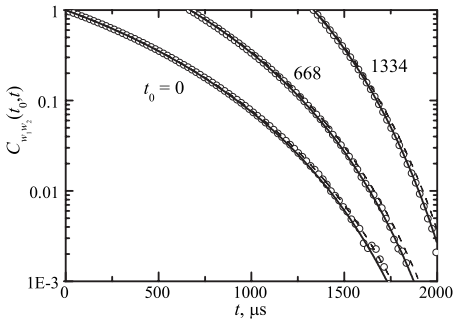

FIG. 4. The VACFs for the rigid+swelling two-reservoir model at the swelling rates $w_1=0$ and $w_2=0.1$ nm/μs are displayed at three different reference times, t_0. In each case, the simulation data are represented as open circles, the linearized treatment obtained by direct replacement of g_1 with G_1 and g_2 with G_2 in Eq. (3.5) is shown as dashed curves, and the perturbative treatment arising from Eqs. (4.1), (4.4), and (3.5) are shown as solid lines.

Assuming that the friction coefficient, $\gamma_{0;1}g_1^2$, is similarly proportional to ν_1, we obtain the expression

$$g_1^2(t) \equiv \frac{\gamma_{0;1}g_1^2(t)}{\gamma_{0;1}g_1^2(0)} = \frac{\nu_1(t)}{\nu_1(0)}. \tag{4.1}$$

The collision frequencies are shown in Fig. 5. For the nonswelling reservoir ν_1 is small during the entire process. The Enskog approximation in Eq. (4.1) should be valid, although ν_1 is not exactly proportional to the particle density even after it is renormalized for the available free volume (dashed line),

$$\rho(t) = \frac{N_1}{L^3 - \frac{4\pi}{3}(R(t)+r_1)^3 - N_2\frac{4\pi}{3}(r_1+r_2)^3}, \tag{4.2}$$

where the denominator is approximately the available volume for the centers of nonswelling spheres. Thus, the collective effect of the hard-sphere binary mixture is connected to the local enhancement in concentration near the tagged particle.

The VACFs shown in Fig. 4 have been fit to a polynomial (as shown in the figure) and results in an overall friction amplitude,

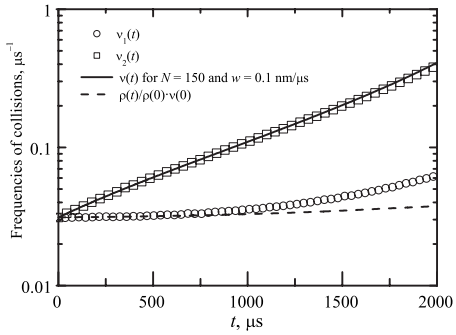

FIG. 5. The frequency of collisions between the tagged particle and bath particles from each reservoir is displayed as function of time during a swelling regime. The open circles correspond to the stationary reservoir with $w_1=0$ and the open squares correspond to the swelling reservoir with $w_2=0.1$ nm/μs. The solid curve is the collision frequency in the one-reservoir case (Sec. IV A) at $w=0.1$ nm/μs. The dashed curve is the relative change in density of nonswelling particles due to the change in available volume, Eq. (4.2) (in arbitrary units).

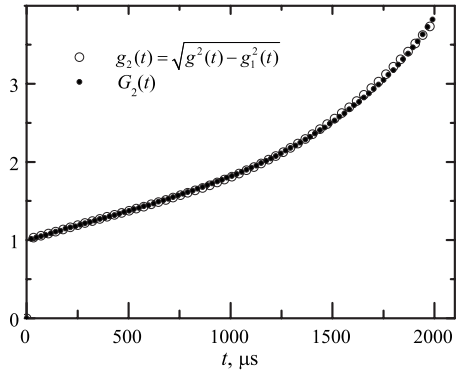

FIG. 6. Comparison between the coupling term g_2 arising from the particle dynamics of the two-reservoir system and the coupling term $G_2(t)$ arising from the linearized approximation in Eq. (4.4) using the one-reservoirs data. [In order to obtain $g_2(t)$, the function $g_1(t)$ must first be obtained after extrapolation along the frequency variable, Eq. (4.1).]

$$g^2 \equiv g_1^2 + g_2^2, \tag{4.3}$$

in accordance with Eq. (3.5). Subtracting g_1^2 [Eq. (4.1)] allows one to obtain the amplitude g_2 for the swelling bath reservoir. On the other hand, the function g_2 for the swelling reservoir in the presence of the nonswelling one can be approximated by the function G_2 corresponding to the case where there is only one swelling bath:

$$g_2(t) \approx G_2(t) \equiv G(r_2(t)). \tag{4.4}$$

This approximation is justified by the fact that the small particles of the unchanging bath reservoir practically do not disturb the dynamics of larger spheres. It can be also seen in Fig. 5 that the frequency of collisions between the tagged sphere and 150 swelling particles in the presence of the rigid ones (squares) coincides with that in the one-reservoir case (Sec. IV A), i.e., in the absence of the rigid spheres (solid line). The comparison of g_2 found using this method and obtained directly from the simulations [Eqs. (4.1) and (4.3)] is presented in Fig. 6. It indicates that the approximation in Eq. (4.4) is reasonable.

In summary, the VACFs for an inhomogeneous mixture of stationary and swelling particles can be obtained from Eq. (3.5). The coupling terms are taken from Eq. (4.4) for the larger particles—g_2—and from Eq. (4.1) for the smaller particles—g_1. The fact that the smaller and larger particles are treated on a different footing should not be cause for alarm. This arises from the observation, illustrated in Fig. 5, that at early times the primary effect on the coupling terms is due to the change in free volume. At longer times, the smaller particles are more sensitive to nonlinearities and hence deviate substantially much sooner than do the bigger particles. Indeed, the overall procedure leads to good agreement with the simulations at various time pairs in the correlation function as shown in Fig. 4 (solid lines). Meanwhile the linearized treatment—in which $G_k(t)$ is used to replace $g_k(t)$ in Eq. (2.14)—gives rise to deviations at long times as seen in the dashed curve of Fig. 4. All of these conclusions can also be drawn from Fig. 7 wherein the swelling rate of the nonstationary reservoir has been doubled.

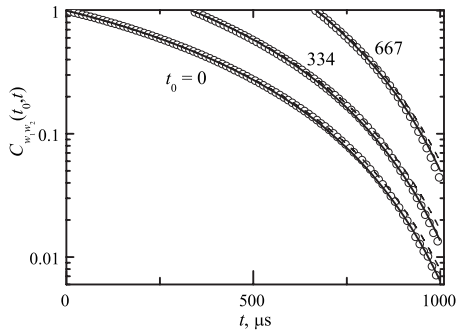

FIG. 7. The VACFs for the rigid+swelling two-reservoir model at the swelling rates $w_1=0$ and $w_2=0.2$ nm/μs are displayed at three different reference times. The swelling rate of the nonstationary bath is twice that for the data in Fig. 4, but all the visual objects retain the same meaning.

C. Two-reservoir response: Homogeneous swelling

The motion of a tagged particle in an environment consisting of $N_1+N_2=300$ homogeneous spheres can also be treated as a two-reservoir system with 150 particles each swelling with the same rate, $w_1=w_2=0.1$ nm/μs. If our approaches are correct, then they should lead to the same result regardless of this fictitious partitioning of the reservoir. Although this case with homogeneous swelling looks simple, actually, it is unfortunately more complicated than the inhomogeneous systems because in the former, both reservoirs are equal in their actions and, thus, it is impossible to make an exact separation of unperturbed/perturbed reservoir dynamics. Nevertheless, it is instructive to consider the approaches described above in the limit of homogeneous swelling.

If the interaction between bath reservoirs is neglected, then $g_k \approx G_k$. Thus, the validity of Eq. (3.5) with g_k replaced with G_k can be checked. Another (better) approximation is based on the rescaling procedure analogous to Eq. (4.1), when the amplitudes are multiplied by the frequency factor,

$$g_k^2(t) \approx G^2(r_k(t))\frac{\nu_k(t)}{\nu(t)}. \tag{4.5}$$

The comparison of these approximations and simulations is shown in Fig. 8. It is remarkable that the linearized and perturbative approximations are effective at early to intermediate times. Of course, the fully coupled system decoheres much more rapidly than the separated models because of the interaction with tertiary particles from different baths.

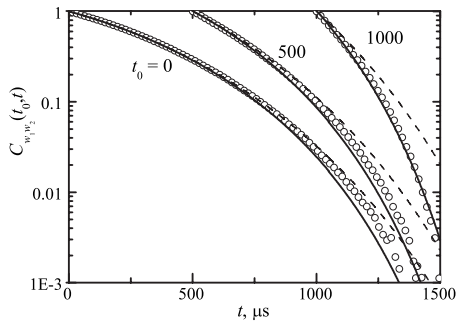

FIG. 8. The VACFs for the homogeneous two-reservoir model at the swelling rates $w_1=w_2=0.1$ nm/μs are displayed at three different reference times. In each case, the simulation data are displayed as open circles, the linearized treatment obtained by setting $g_k(t)=G_k(t)$ in Eq. (3.5) is shown as a dashed curve, and the perturbative treatment obtained from Eq. (3.5) with g_k^2 from Eq. (4.5) is shown as a solid curve.

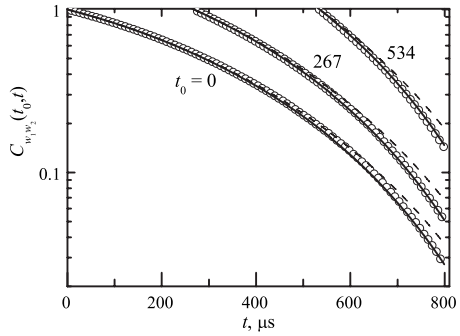

FIG. 9. The VACFs for the inhomogeneous two-reservoir model at the swelling rates $w_1=0.1$ and $w_2=0.2$ nm/μs are displayed at three different reference times. In each case, the simulation data are displayed as open circles, the linearized treatment obtained by setting g_1 with G_1 in Eq. (3.5) is shown as a dashed curve, and the perturbative treatment obtained from Eqs. (4.6), (4.7), and (3.5) is shown as a solid curve.

D. Two-reservoir response: Inhomogeneous swelling

Finally, we consider a case in which both baths swell, but at different rates. Each bath consists of 150 particles, but the swelling rate of the first reservoir is $w_1=0.1$ nm/μs, whereas that of the second one is $w_2=0.2$ nm/μs. The case when both reservoirs nonsynchronously change with time is the most complicated for the analysis. However, the linearized and perturbative treatments employed in the previous cases can be combined to address the inhomogeneous swelling system.

We assume that the bath consisting of smaller particles—relabeled as bath 1—affects the interaction between the tagged particle and the larger particles—relabeled as bath 2—weakly, if at all. Thus the amplitude for the interaction to the larger particles can be approximated by a one-parameter term,

$$g_2(t) \approx G(r_2(t)), \tag{4.6}$$

calculated at a corresponding macrostate parametrized by the particles' radius $r_2(t)$. The influence of the small particles can be treated using the rescaling procedure from Eq. (4.5):

$$g_1^2(t) \approx G^2(r_1(t))\frac{\nu_1(t)}{\nu(t)}, \tag{4.7}$$

where $G(r_1)$ is an amplitude of a one-reservoir bath swelling at the corresponding rate, w_1, $\nu_1(t)$ is the frequency of collisions between the tagged sphere and small particles, and $\nu(t)$ is the frequency of collisions between the tagged sphere and small particles in the absence of the second bath reservoir. The last quantity is shown in Fig. 3 and depends only on the state of the subsystem which is characterized by r_1, i.e., $\nu(t) \equiv \nu(r_1(t))$.

The results of numerical simulations of the inhomogeneous swelling case are presented in Fig. 9. The linearized treatment based on the one-dimensional functions $G_1(t) \equiv G(r_1(t))$ and $G_2(t) \equiv G(r_2(t))$ instead of $g_1(t)$ and $g_2(t)$ in Eq. (3.5) gives worse results than the perturbative treatment.

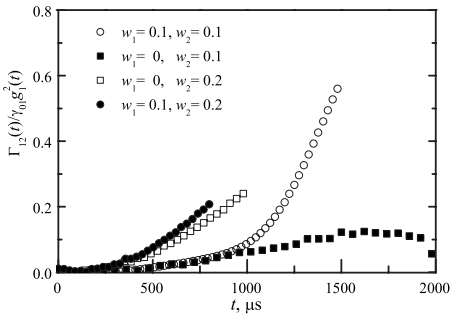

FIG. 10. Relations of the bath-bath correlation function, $\Gamma_{12}(t)$, to the smallest friction coefficient, $\gamma_{0;1}g_1^2(t)$, as functions of time for all two-reservoir simulations (the swelling rates are in nm/μs).

If the coupling between the reservoirs were stronger, then one must use a projected iLE model, like that in Eq. (2.13), that is generalized to include auxiliary stochastic equations for each of the reservoirs. It includes direct and dissipative interactions between the baths that are captured in the correlation function $\Gamma_{12}(t)$ between particles from each reservoir. The magnitudes of this bath-bath correlation, Γ_{12}, for the homogeneous and inhomogeneous systems are calculated using Eq. (2.15) and shown in Fig. 10. In the inhomogeneous case, the values are clearly small throughout. In the homogeneous swelling case, the two-bath reservoirs must affect each other equally. Figure 10 justifies the perturbative treatment in the case of small Γ_{12}, in the framework of which the amplitude functions g_k obtained from the unperturbed ones, G_k, by use of the rescaling procedure work better. Thus, at least for the current cases of reservoir coupling, the separation of the bath reservoirs can be treated perturbatively within a reduced dimensional framework.

V. CONCLUDING REMARKS

The diffusion of a large heavy colloid immersed within a binary mixture of swelling (nonstationary) particles has been investigated. The particles from each component hard sphere gas swell at a given rate and can be represented collectively as a nonequilibrium bath reservoir. The extended version of the iLE, which allows for a complex structure in the nonequilibrium environment, appears to be an adequate description of the process.

To adapt the iLE to this particular problem, the information about the nonstationary amplitude $g(t)$ of the stochastic noise is necessary. This amplitude can be composed of two others, G_1 and G_2, which define the behavior of the tagged particle in each subenvironment separately. The overall function $g(t)$ is obtained after subsequent rescaling of the functions G_1 and G_2 to account for their dependence on the state of the environment in the immediate vicinity to the tagged sphere. In MD simulations, the functions g, G_1 and G_2 can be found by the direct extraction of quantities—the mean square displacement or the VACF—which are available when one keeps track of every particle. The nonstationary amplitudes can also be inferred from experiments by way of inverting diffusional data, structure functions, or energy correlation functions.

In an inhomogeneous swelling system, one of the amplitudes—the one for larger particles—can be approximated by that from the neat one-reservoir case. This approximation succeeds because of the negligible influence exerted by the other bath reservoir onto the larger bath. Meanwhile the coupling amplitude between the tagged particle and the smaller bath needs to be rescaled because the local composition of smaller particles around the probe is affected by the larger particles [although it is not quite linear with its overall density, $\rho(t)$]. Thus, it has been shown that—at least for a binary mixture of hard spheres—the composition rule (4.3) allows one to restore the coupling amplitude $g(t)$ without requiring detailed recalculations of the kinetic coefficients for the whole process in response to a changing (nonstationary) environment.

ACKNOWLEDGMENTS

This work has been supported by the National Science Foundation through Grant Nos. NSF 04-43564 and 07-49580.

[1] R. Hernandez and F. L. Somer, J. Phys. Chem. B **103**, 1064 (1999).
[2] R. Hernandez, J. Chem. Phys. **111**, 7701 (1999).
[3] A. V. Popov, J. Melvin, and R. Hernandez, J. Phys. Chem. A **110**, 1635 (2006).
[4] A. V. Popov and R. Hernandez, J. Chem. Phys. **126**, 244506 (2007).
[5] R. Hernandez and F. L. Somer, J. Phys. Chem. B **103**, 1070 (1999).
[6] M. Vogt and R. Hernandez, J. Chem. Phys. **123**, 144109 (2005).
[7] J. M. Moix, T. D. Shepherd, and R. Hernandez, J. Phys. Chem. B **108**, 19476 (2004).
[8] C. D. Jones and L. A. Lyon, Macromolecules **33**, 8301 (2000).
[9] J. Wang, D. Gan, L. A. Lyon, and M. A. El-Sayed, J. Am. Chem. Soc. **123**, 11284 (2001).
[10] C. D. Jones and L. A. Lyon, Macromolecules **36**, 1988 (2003).
[11] A. Fernández-Nieves, A. Fernández-Barbero, B. Vincent, and F. J. de las Nieves, Prog. Colloid Polym. Sci. **115**, 134 (2000).
[12] M. J. Garcia-Salinas, M. S. Romero-Cano, and F. J. de las Nieves, Prog. Colloid Polym. Sci. **118**, 180 (2001).
[13] A. Fernández-Nieves, A. Fernández-Barbero, and F. J. de las Nieves, J. Chem. Phys. **115**, 7644 (2001).
[14] A. Fernández-Nieves, A. Fernández-Barbero, B. Vincent, and F. J. de las Nieves, Macromolecules **33**, 2114 (2000).
[15] A. Fernández-Nieves, A. Fernández-Barbero, B. Vincent, and F. J. de las Nieves, J. Chem. Phys. **119**, 10383 (2003).
[16] R. Pelton, Adv. Colloid Interface Sci. **85**, 1 (2000).
[17] A. Fernández-Barbero, A. Fernández-Nieves, I. Grillo, and E. López-Cabarcos, Phys. Rev. E **66**, 051803 (2002).
[18] R. Zwanzig, *Nonequilibrium Statistical Mechanics* (Oxford University Press, London, 2001).
[19] M. C. Mahato, T. P. Pareek, and A. M. Jayannavar, Int. J. Mod. Phys. B **10**, 3857 (1996).
[20] A. Jayannavar and M. C. Mahato, Pramana, J. Phys. **45**, 369 (1995).
[21] M. M. Millonas and C. Ray, Phys. Rev. Lett. **75**, 1110 (1995).
[22] J. R. Chaudhuri, G. Gangopadhyay, and D. S. Ray, J. Chem. Phys. **109**, 5565 (1998).
[23] J. R. Chaudhuri, S. K. Banik, B. C. Bag, and D. S. Ray, Phys. Rev. E **63**, 061111 (2001).
[24] J. R. Chaudhuri, D. Barik, and S. K. Banik, Phys. Rev. E **73**, 051101 (2006).
[25] J. R. Chaudhuri, S. Chattopadhyay, and S. K. Banik, J. Chem. Phys. **127**, 224508 (2007).
[26] G. R. Kneller and G. Sutmann, J. Chem. Phys. **120**, 1667 (2004).
[27] M. Shibayama and K. Nagai, Macromolecules **32**, 7461 (1999).
[28] S. Chapman and T. G. Cowling, *The Mathematical Theory of Non-uniform Gases* (Cambridge University Press, New York, 1995).